GEOPHYSICS, VOL. 48, NO. 9 (SEPTEMBER 1983); P. 1212–1218. 7 FIGS., 1 TABLE

Localized heat flow and Tertiary mineralization in southern New Mexico

Gary W. Zielinski* and Gail Moritz DeCoursey‡

ABSTRACT

Eight shallow (< 100 m deep) relative heat flow determinations from southern New Mexico reveal a systematic 3 HFU (125 mW/m^2) increase occurring within a distance of 2 km. The maximum surface heat flow appears roughly to overlie a Tertiary granitic body at a depth of about 600 m within an area of known hydrothermal mineralization. The presence of the anomaly, believed to be of subsurface origin, implies an active heat source centered at a depth of 1140 m, perhaps associated with hydrothermal circulation. Higher radioactive heat production in granites may contribute to convective instability and explain the apparent lateral coincidence between the anomaly and the body. This situation appears, on a local scale, analogous to coinciding zones of high present-day heat flow and mineralization in England and Wales (Brown et al, 1980). In both cases, mineralization is associated with granitic intrusion that has occurred at a previous time which is much greater than the thermal time constant for cooling bodies. Shallow heat flow determinations may be useful in locating other similar areas and investigating possible associations of mineralization and thermal history.

INTRODUCTION

Cenozoic volcanism and concomitant mineralization is a well-established and widespread feature of the geology of New Mexico (Lindgren et al, 1910; Lasky and Wooton, 1933; Talmage and Wooton, 1937; Callaghan, 1953; Northrop, 1959). Our study area, encompassing roughly 30 km^2 in southern New Mexico, comprises a local example of this occurrence. The area consists of a group of east-west trending ridges of sedimentary and volcanic rock rising more than 200 m above a broad plain of Tertiary and Quaternary alluvium. From information provided by Gulf Mineral Resources Company, the sedimentary sequence in the area consists predominately of Paleozoic carbonates reaching a thickness of over 500 m. Extrusive volcanic activity began in the Early Cretaceous and culminated in the Middle Tertiary with the emplacement of a granitic pluton, an apophysis of which is exposed nearby. Hydrothermal mineral deposits, including varying concentrations of gold, silver, copper, lead, and zinc, recognized prior to 1880, exist in small but commercial quantities.

Compilations of terrestrial heat flow data from New Mexico (Reiter et al, 1975; Edwards et al, 1978; Shearer and Reiter, 1981) indicate generally above average and variable heat flow. This is largely attributed to varying amounts of Cenozoic magmatism, hydrothermal circulation, and radioactive heat production in the crust. In order to investigate the present-day thermal regime in our study area in relation to local volcanism and mineralization, a suite of 8 shallow (~35 m) relative heat flow determinations was attempted in November, 1980. The particular location of the measurements was based on the availability of subsurface data from previous deep drilling. It was hoped that these determinations might reveal some additional information on the area's thermal history; at the same time, the uncertainties as well as the potential of shallow land-based heat flow measurements could be explored.

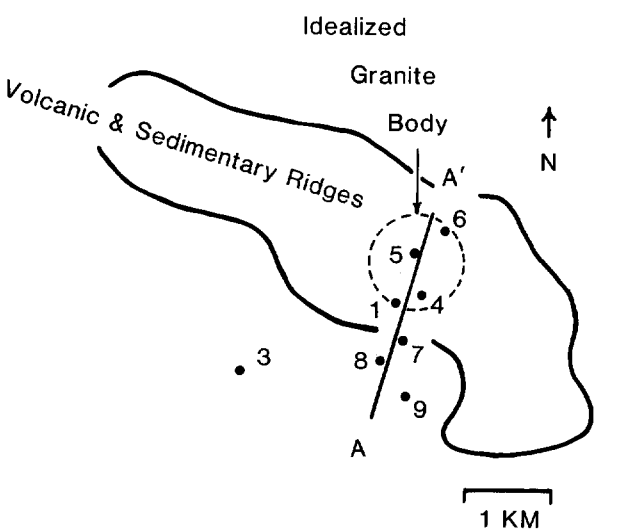

FIG. 1. Relative position of heat flow stations (numbered dots), the local zone of volcanic and sedimentary topographic relief and an idealized granite body (dashed circle) for the study area in southern New Mexico.

Manuscript received by the Editor August 19, 1982; revised manuscript received December 29, 1982.
*Dept. of Geochemistry and Minerals, Gulf Research and Development Company, P.O. Drawer 2038, Pittsburgh, PA 15230.
‡Formerly Dept. of Geological Sciences, University of Rochester, Rochester, NY 14627; presently Marathon Oil Company, P.O. Box 3128, Houston, TX 77001.

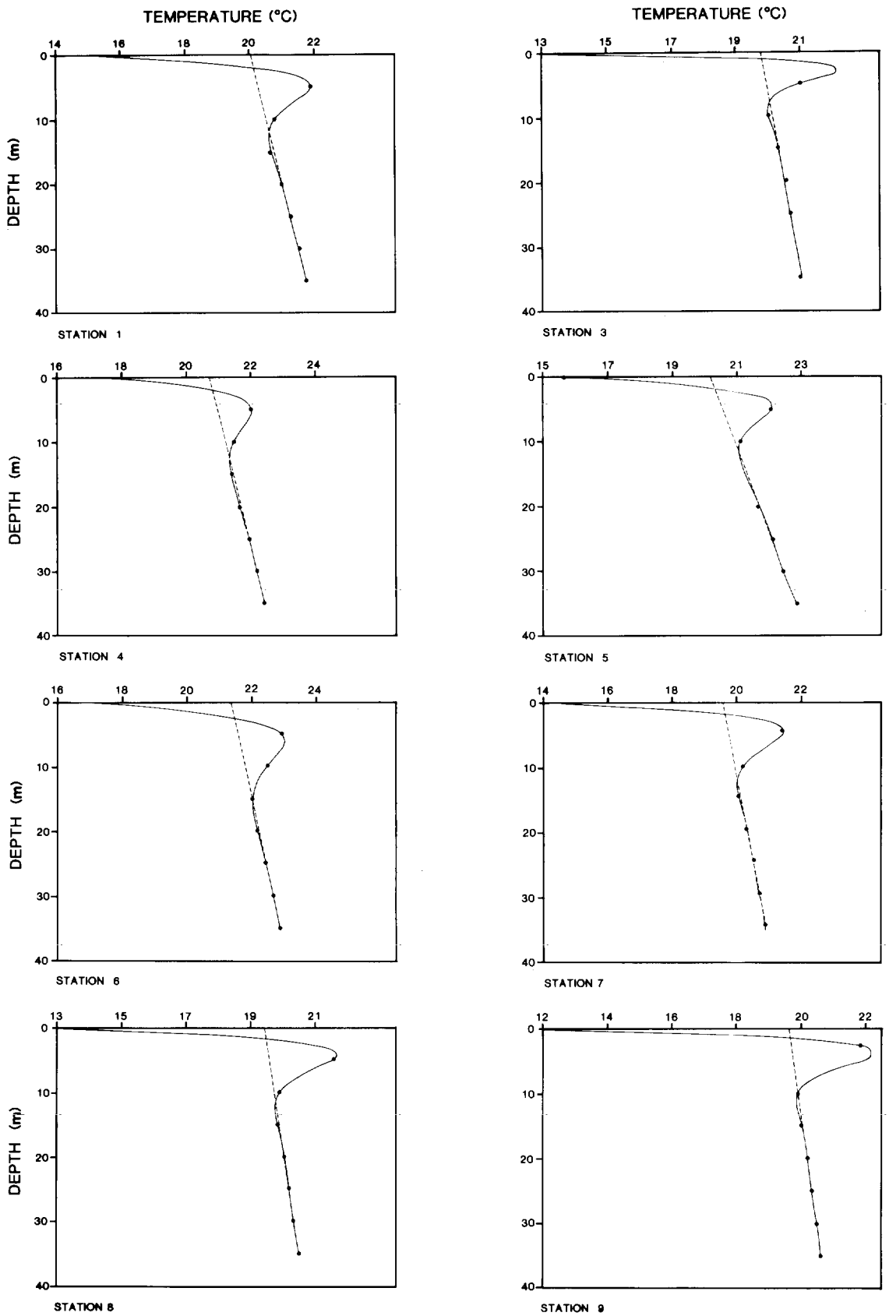

FIG. 2. Observed temperatures (dots) and calculated temperatures (solid curves) for the heat flow stations versus depth. Dashed lines represent estimated geothermal gradients from regression.

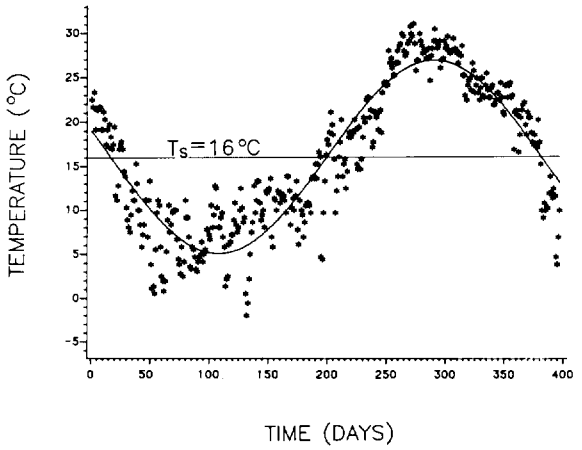

FIG. 3. Observed surface air temperatures for the study area in southern New Mexico, from October 1, 1979 (day 0) to October 31, 1980 (day 396). The solid curve is the best fit sinusoid.

MEASUREMENTS

The orientation of the heat flow stations, given in Figure 1, is roughly perpendicular to the principal topographic trend. Measurements were made in the upper 35 m of thermally equilibrated boreholes. These were accomplished by lowering a thermistor probe into each borehole and obtaining equilibrated readings from 5 to 35 m in 5 m increments. The thermistor output was monitored with a digital ohm-meter operating in the 4-wire mode and converted to temperature by a previously determined calibration function (Steinhart and Hart, 1968). Considerable laboratory testing of the measurement system against a platinum resistance thermometer and resistance bridge allows estimates of absolute accuracy at about 0.02°C and relative error at <0.002°C. Because of the long equilibration time of the thermistor probe, only 2 sites could be completed per day resulting in a total 4 day sampling period. The results of these measurements are shown in Figure 2 (black dots).

The temperature values shown in Figure 2 were obtained in a depth interval where it is likely that the dominant transient component of the temperature field results from the seasonal fluctuation of surface temperature. The indirect method of Lee (1977) was used to remove this transient component from the temperature profiles and to obtain an estimate of the mean equilibrium geothermal gradient and a value of the average thermal diffusivity over the depth interval for each station. More specifically, the procedure uses a linearized form of the solution for heat conduction in a homogeneous half-space with sinusoidally varying surface temperature (period = 1 year),

$$T_{ji} = T_s + gz_i + \delta_j x_i + \varepsilon_j y_i \quad (1)$$

where

$$\delta_j = A \sin \omega(t_j - t_0),$$

$$\varepsilon_j = -A \cos \omega(t_j - t_0),$$

and

$$x_i = \exp(-z_i\sqrt{\omega/2\mu}) \cos(z_i\sqrt{\omega/2\mu}),$$

$$y_i = \exp(-z_i\sqrt{\omega/2\mu}) \sin(z_i\sqrt{\omega/2\mu}).$$

T_{ji} are the temperatures measured at depth z_i at time t_j, T_s is the mean surface temperature, A is the amplitude of the annual surface temperature variation, g is the geothermal gradient, ω is the angular velocity of the annual temperature variation (2×10^{-7} sec^{-1}), t_0 is the time when $T(z = 0) = T_s$, and μ is thermal diffusivity. A minimum root-mean-square (rms) error solution to equation (1) is sought after assigning discrete values of μ ranging from 0.001 to 0.020 cm^2/sec in increments of 10^{-4} cm^2/sec, which covers the range of values normally observed for most soils and rock (Kappelmeyer and Haenel, 1974). Corresponding best-fit values of μ and g are assumed to be the correct values. The data in Figure 2, however, were not adequate to obtain a best-fit solution to equation (1) by the indirect method of Lee (1977) without imposing one additional constraint. This was obtained from daily surface air temperature measurements (recorded at a U.S. Weather Service station located 55 km away) for a period of 1 year prior to our field measurements (Figure 3). The solid curve in Figure 3 is the best-fit sinusoid (period = 1 year) to the data. This allows an estimate of t_0 and hence $t_j - t_0$ could be specified in equation (1) for each station assuming there is no difference in phase between the annual air temperature and ground temperature fluctuations at the surface.

The results of reduction of the temperature data in Figure 2 are summarized in Table 1. The theoretical temperature profiles corresponding to the parameters in Table 1 are plotted along with the data in Figure 2 (solid curves). The dashed lines in Figure 2 indicate the computed geothermal gradient for each station resulting from removal of the periodic component from the temperature data. Based on the values of the coefficient of determination R^2 obtained (Table 1), there is in general a good fit ($R^2 = 1$ would indicate a perfect fit) of the data to the assumed conductive theory [equation (1)]. The values of T_s in Table 1 average about 4°C higher than the mean annual air temperature (Figure 3). This is no doubt the result of direct radiative heating of the ground. (The air temperatures were recorded in a covered shed.) Because of this effect, Kappelmeyer and Haenel (1974) stated that workers often recommend the

Table 1. Summary of thermal results.

Station	μ	g	T_s	A	R^2	K	q
1	10.5	5.10	20.01	9.31	.9996	5.71	2.91
3	4.1	3.59	19.82	12.51	.9924	3.02	1.08
4	12.9	4.91	20.72	5.86	.9996	6.72	3.30
5	10.1	7.72	20.18	8.60	.9992	5.54	4.28
6	16.7	4.38	21.39	7.82	.9995	8.31	3.64
7	10.0	3.81	19.57	9.32	.9999	5.50	2.09
8	8.7	3.07	19.43	11.52	.9998	4.95	1.52
9	6.7	2.94	19.54	14.33	.9993	4.11	1.21

μ = Thermal diffusivity ($\times 10^{-3}$ cm^2 sec^{-1})
g = Geothermal gradient ($\times 10^{-4}$ °C cm^{-1})
T_s = Mean surface temperature (°C)
A = Amplitude of the surface temperature change (°C)
R^2 = Coefficient of determination
K = Thermal conductivity ($\times 10^{-3}$ cal °C^{-1} cm^{-1} sec^{-1})
q = Heat flow ($\times 10^{-6}$ cal cm^{-2} sec^{-1})

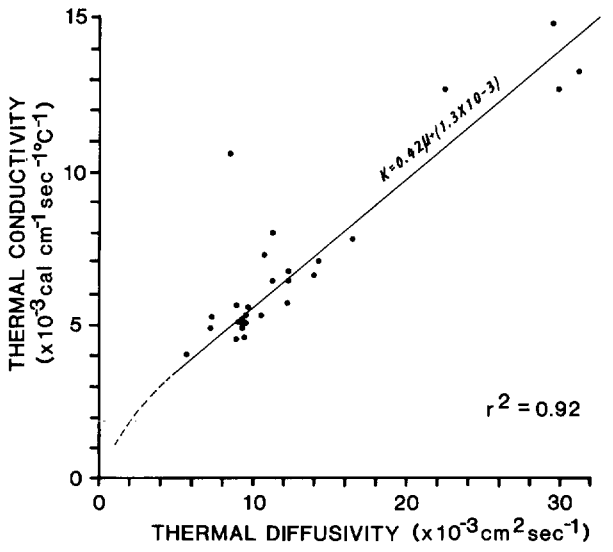

FIG. 4. Relationship between thermal diffusivity and thermal conductivity. Dots are data for solid rock taken from Kappelmeyer and Haenel (1974) and the straight line is the least-squares fit to the data. The dashed line is an empirical representation of thermal diffusivity versus thermal conductivity for unconsolidated ocean bottom sediment derived from Bullard (1963).

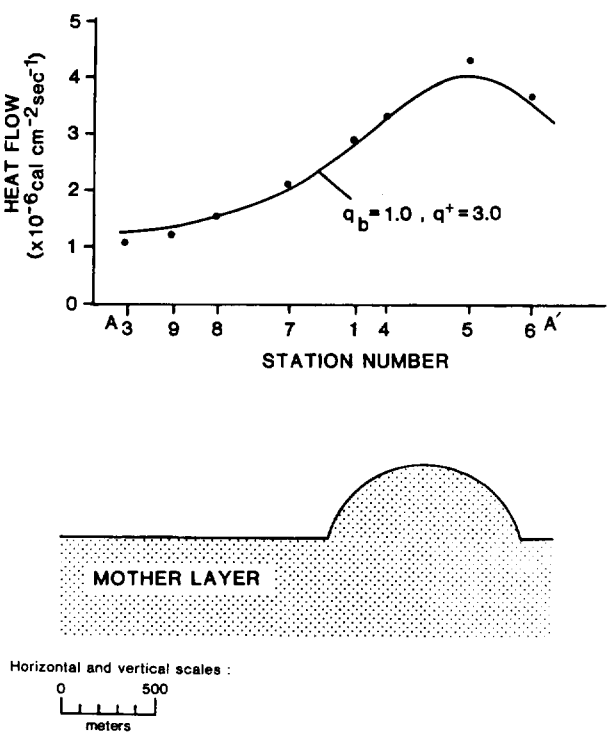

FIG. 5. Observed (dots) and theoretical heat flow (curve) along section A-A′ in Figure 1. q_b is background heat flow and q^+ is the additional heat flow from a spherical source. Below is the simplified geometry of a subsurface granitic body. Depth and lateral extent are based on information from deep boreholes.

rule of thumb addition of 1°C to the mean annual air temperature to estimate mean ground temperature. Clearly, from Table 1, this difference can be significantly larger. The site-to-site variation in T_s (Table 1) is most likely due to differences in the exposure of the ground to incident solar radiation since differences in albedo caused by variations in ground cover over the area are probably insignificant.

For most of the stations the lithology corresponding to the temperature measurement interval comprised undifferentiated Quaternary gravel, soil, and alluvium. The values of μ obtained from the data reduction (Table 1) are therefore highly variable, as might be expected; however, for station 1 and possibly station 7 measurements were obtained in dolomite. These are in excellent agreement with measured values reported in the literature (Kappelmeyer and Haenel, 1974). The values of μ in Table 1 were used to obtain a rough estimate of thermal conductivity K for each station. This was done by plotting average values of thermal conductivity versus average thermal diffusivity for a wide range of lithologies (Figure 4). The data are from the compilation of Kappelmeyer and Haenel (1974). Included also is a theoretical relation (dashed curve) for unconsolidated sediments (Bullard, 1963). A least-squares line fit to the data over the range appropriate for consolidated rocks leads to the relation $K = 1.3 \times 10^{-3} + 0.42\ \mu$ which was used to compute the thermal conductivity given in Table 1. Implicit in this procedure is the assumption that, over the range appropriate to consolidated rocks, variations in the density and heat capacity of rocks are small compared with variations in thermal conductivity. The data in Figure 4 sufficiently support this assumption for the present purposes. This estimate of K in turn allows an estimate of relative heat flow $q = Kg$ for each site, which is also given in Table 1.

Transient temperature disturbances caused by thermal convection within the boreholes (Diment, 1967; Gretener, 1967) cannot be ruled out a priori for the temperature data in Figure 2. This effect does not, however, appear to present a problem to the data set in general. The level of agreement of the data set to conductive theory (Figure 2 and Table 1) and the uniformity of computed parameters (Table 1) do not suggest the presence of serious random temperature perturbations, particularly in view of the sizeable and remarkably systematic trend observed in the heat flow values, which will be seen in the next section.

RESULTS

The results of the heat flow estimates for each station (Table 1) are plotted in Figure 5 as a function of relative position projected on line A-A′ (Figure 1). The lower section of Figure 5 shows the suggested position of a subsurface granitic body (Figure 1) approximated by a hemisphere. The approximate depth and lateral extent of the granite as well as its approximate location with respect to the heat flow measurements are based on information from deep boreholes provided by Gulf Mineral Resources Company. The continuity of the body and the existence of the mother layer are somewhat speculative and largely for the purpose of the heat flow interpretation.

The relative heat flow values in Figure 5 exhibit a large and systematic increase as the ridge province (Figure 1) is approached from the south-southwest. The maximum observed increase in relative heat flow of 3 HFU (1 HFU = 10^{-6} cal cm^{-2} sec = 41.8 mW/m^2) appears to be centered around station 5. Since the magnitude of the observed increase is too large to be accounted for by heat conduction effects of

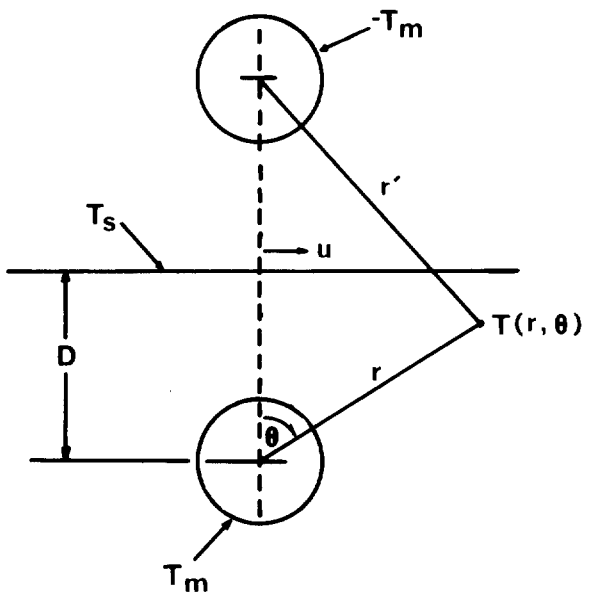

FIG. 6. Geometry for applying the method of images to a buried sphere.

surface topography, nor does it relate to individual station elevation or slope orientation, a subsurface cause must be responsible.

Hardee and Larson (1980) arrived at a relation for the steady state surface heat flow as a function of horizontal position u for a sphere of radius a at constant temperature T_m, buried at depth D in a medium initially at zero temperature, with a horizontal surface held at constant temperature T_s (see Figure 6). Their result was that

$$\frac{q}{q^+} = \left[1 + \left(\frac{u}{D}\right)^2\right]^{-2}, \tag{2}$$

where

$$q^+ = -\frac{2aK(T_m - T_s)}{D^2}, \tag{3}$$

is the maximum heat flow (at $r = D$, $\theta = 0$). The solid curve in Figure 5 is the result of applying equations (2) and (3) to the heat flow data. Equation (2) was used to estimate from the data the depth D to the center of a spherical source capable of creating the observed anomaly ($D = 1140$ m). The heat flow values at stations 3 and 9 suggest a background heat flow $q_b (u \to \infty)$ of about 1 HFU so that a value of $q^+ \cong 3$ HFU is then required to fit the observations near the crest of the anomaly. From equation (3), for example, a temperature excess of 50°C (for $K = 7$ mcal °C^{-1} cm^{-1} sec^{-1}), its position and depth coinciding with the surface of the granitic body illustrated in Figure 5, would produce the theoretical heat flow profile (solid curve) in Figure 5, which is in excellent agreement with the measurements. This result suggests a possible association between the granite body and the observed relative heat flow. Furthermore, it is clear from the magnitude of the required temperature excess that heat conduction effects resulting from possible contrasts in thermal properties and radioactive heat production (between the granite and surrounding rock) alone are incapable of accounting for the observed anomaly.

In order to test the possibility that the suggested temperature excess is the result of transient cooling of the body from an originally molten state, we have applied the method of images to a sphere cooling from some initial temperature T_m. From the solution for an infinite region,

$$T(r, t) = \frac{T_m}{2}\left(\operatorname{erf}\frac{r+a}{2\sqrt{\mu t}} - \operatorname{erf}\frac{r-a}{2\sqrt{\mu t}} - \frac{2\sqrt{\mu t}}{r\sqrt{\pi}} \cdot \{\exp[-(r-a)^2/4\mu t] - \exp[-(r+a)^2/4\mu t]\}\right) \tag{4}$$

(Carslaw and Jaeger, 1959), the solution for a semi-infinite medium (Figure 6) becomes

$$T(r, t) = \frac{T_m}{2}\left\{\operatorname{erf}\frac{r+a}{2\sqrt{\mu t}} - \operatorname{erf}\frac{r-a}{2\sqrt{\mu t}} - \frac{2\sqrt{\mu t}}{r\sqrt{\pi}} \cdot \{\exp[-(r-a)^2/4\mu t] - \exp -(r+a)^2/4\mu t\}\right\} - \frac{T_m}{2}\left\{\operatorname{erf}\frac{r'+a}{2\sqrt{\mu t}} - \operatorname{erf}\frac{r'-a}{2\sqrt{\mu t}} - \frac{2\sqrt{\mu t}}{r'\sqrt{\pi}} \cdot \{\exp[-(r'-a)^2/4\mu t] - \exp[-(r'+a)^2/4\mu t]\}\right\}, \tag{5}$$

where

$$r' = [r^2 + 4D^2 - 4rD\cos\theta]^{1/2}.$$

The solution for heat flow q is

$$q = -K\left.\frac{dT}{dr}\right|_{\theta=0} = -KT_m \exp\left(-\frac{(D+a)^2}{4\mu t}\right)\left[\frac{1}{\sqrt{\pi\mu t}} - \frac{a+D}{D\sqrt{\pi\mu t}} - \frac{2\sqrt{\mu t}}{D^2\sqrt{\pi}}\right] + T_m \exp\left(-\frac{(D-a)^2}{4\mu t}\right)\left[\frac{-1}{\sqrt{\pi\mu t}} - \frac{a+D}{D\sqrt{\pi\mu t}} + \frac{2\sqrt{\mu t}}{D^2\sqrt{\pi}}\right]. \tag{6}$$

In Figure 7 we have plotted heat flow versus time from equation (6) for a cooling sphere with $T_m = 1000$°C, $K = 7$ mcal °C^{-1} cm^{-1} sec^{-1}, $\mu = 0.01$ cm^2 sec^{-1}, and the approximate observed dimensions (inset) which correspond to Figure 5. First seen (Figure 7) is a buildup of heat flow as heat from the buried sphere reaches the surface and then a decrease as that heat is eventually lost. The important result, however, is that all this occurs within 100,000 years. Thus, if the granite body, approximated by a sphere, is of Tertiary age, no residual heat flow would be expected to remain at present time. Our theoretical treatment of the cooling granite body neglects possible cooling by convective heat transfer. However, incorporating convection in our model would decrease the estimated cooling time and, therefore, would not alter our conclusion.

It is also possible to speculate on the existence of a somewhat deeper mother layer (Figure 5) of considerable lateral extent as a source of residual transient heat flow. The heat flow solution for a cooling, buried half-space (used to represent a cooling granitic batholith in Goguel, 1976), given by

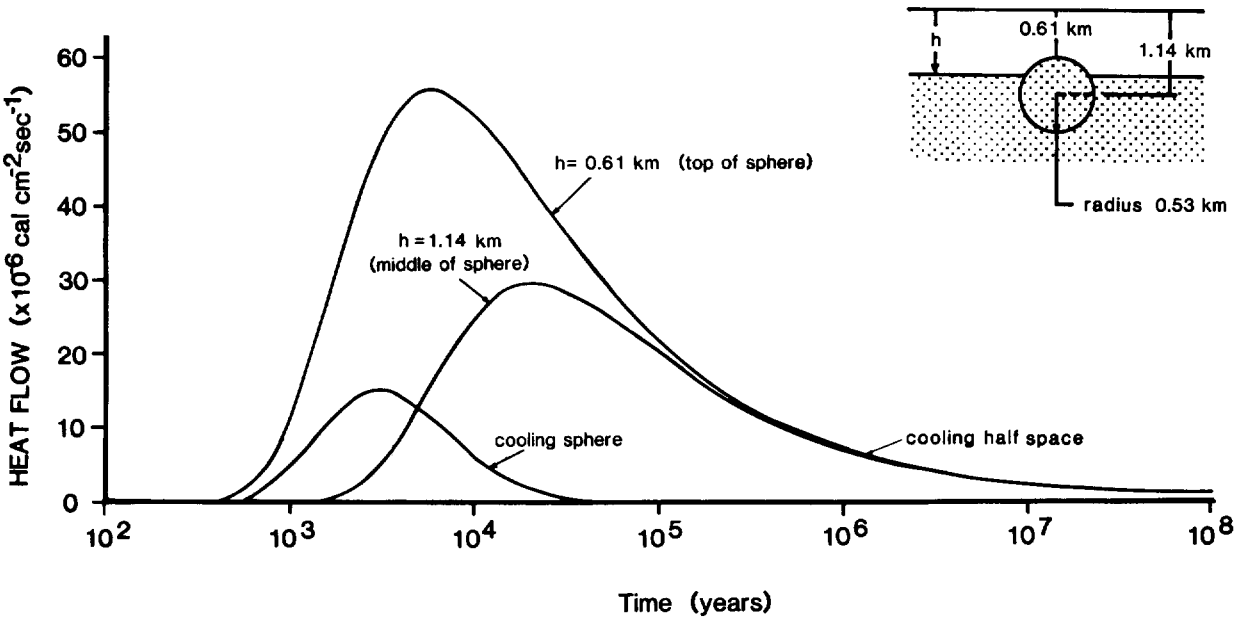

FIG. 7. Theoretical cooling of a buried half-space (at depth h) and cooling sphere. Dimensions and geometry are inset.

$$q = \frac{-2KT_m}{2\sqrt{\pi\mu t}} \exp(-h^2/4\mu t), \quad (7)$$

was used to explore this possibility. These results are also plotted in Figure 7 for the same parameters as the cooling sphere but for depths $h = 610$ m (corresponding to the top of the sphere) and $h = D = 1140$ m. In both cases (Figure 7) significant residual heat flow remains after 10^7 years. Thus a mother layer cooling from mid-Tertiary time is capable of supplying enough heat to account for the observed q^+ of 3 HFU. Still, transient cooling of a smaller wavelength granite body as a mechanism is insufficient to account for the shape of the observed heat flow anomaly even if heat is supplied by the mother layer. The effect of the thermal conductivity contrast between granite and limestone or dolomite is far too small (Lovering, 1935) to offset the rapid cooling time of a sphere or hemisphere of an appropriate size (Figures 5 and 7).

Based on these results, it must be concluded that the heat flow anomaly observed in the study area is not the direct result of transient cooling of a granite body, but must be indicative of an active (or recently active) process such as hydrothermal circulation. The heat flow estimated for stations 3 and 9, 1.08 and 1.21 HFU, is less than most published values from the surrounding area, ~2.0 HFU (Reiter et al, 1975; Edwards et al, 1978; Shearer and Reiter, 1981). Although the absolute accuracy of the shallow heat flow determinations in Table 1 is not well established, the range of values does not significantly depart from that observed via deep borehole observations in areas of extensive volcanic activity in northeastern New Mexico and southeastern Colorado (Edwards et al, 1978). The low background heat flow ($q_b = 1$ HFU) suggested earlier could imply low reduced heat flow as well as a low contribution from crustal radioactive heat production. Leaching of radioactive elements by moving groundwater has been suggested to explain locally nonrepresentative crustal radioactivity in Arizona (Shearer and Reiter, 1981). In that same study, forced and free convection by moving groundwater was called upon to explain some of the variability of heat flow measurements taken shallower than 650 m. The heat flow pattern shown in Figure 5 also might be the result of a local redistribution of heat by hydrothermal convection occurring at depth. In this case the low values at stations 3 and 9 could be indicative of removal of heat as in the case of a downgoing limb of a convection cell. Higher concentrations of heat-producing elements in the granite body, while incapable of producing 3 HFU to cause the observed anomaly, may contribute to the convective instability. Such a mechanism might focus the convection and explain the location of the heat flow high over the granite body.

CONCLUSIONS

There appears to be spatial coincidence between a present-day heat flow anomaly, a Tertiary granitic body, and hydrothermal mineralization within a localized area in southern New Mexico. Based on the heat flow values obtained, hydrothermal circulation is believed to be the most likely explanation for the heat flow anomaly. Higher radioactive heat production in the granite body may explain the spatial coincidence between the anomaly and the body. The situation appears analogous to the regional association between zones of high heat flow, metalliferous mineralization, and intrusive bodies in England and Wales (Brown et al, 1980). There it was postulated that Caledonian age intrusive bodies focused the development of hydrothermal systems responsible for post-Carboniferous mineralization, and that these systems have persisted through time to create the present-day high heat flow.

Our results suggest the possibility of such occurrences on a local scale and the potential of shallow thermal measurements as an aid in locating and understanding them.

ACKNOWLEDGMENTS

The authors wish to thank Tom Heidrick, Jerzy Maciolek, Ian Lerche and two anonymous reviewers for helpful comments which led to improvements in the original manuscript. We also thank Gulf Oil Corporation for permission to publish the heat flow data and Tom Heidrick for encouraging us to make the measurements.

REFERENCES

Brown, G. C., Cassidy, J., Oxburgh, E. R., Plant, J., Sabine, P. A., and Watson, J. V., 1980, Basement heat flow and metalliferous mineralization in England and Wales: Nature, v. 288, p. 657–659.

Bullard, E. C., 1963, The flow of heat through the floor of the ocean, *in* The Sea: M. Hill, Ed., v. 3, p. 218–232.

Callaghan, E., 1953, Volcanic rocks of southwestern New Mexico: N. Mex. Geol. Soc., 4th Field Conference.

Carslaw, H. S., and Jaeger, J. C., 1959, Conduction of heat in solids: Oxford University Press, Oxford.

Diment, W. H., 1967, Thermal regime of a large diameter borehole: Instability of the water column and comparison of air- and water-filled conditions: Geophysics, v. 32, p. 720–726.

Edwards, C. L., Reiter, M., Shearer, C., and Young, W., 1978, Terrestrial heat flow and crustal radioactivity in northeastern New Mexico and southeastern Colorado: GSA Bull., v. 89, p. 1341–1350.

Goguel, J., 1976, Geothermics: New York, McGraw-Hill Book Co.

Gretener, P. E., 1967, On the thermal instability of large diameter wells—An observational report: Geophysics, v. 32, p. 727–738.

Hardee, H. C., and Larson, D. W., 1980, Thermal techniques for characterizing magma body geometrics: Geothermics, v. 9, p. 237–249.

Kappelmeyer, O., and Haenel, R., 1974, Geothermics with special reference to application: Geoexploration Monographs, series 1, no. 4, Gebrüder Borntraeger, Berlin.

Lasky, S. G., and Wooton, T. P., 1933, The metal resources of New Mexico and their economic features: N. Mex. School of Mines, State Bur. Mines and Mineral Res. Bull. 7.

Lee, T-C., 1977, On shallow-hole temperature measurements—A test study in the Salton Sea geothermal field: Geophysics, v. 42, p. 572–583.

Lindgren, W., Graton, L. C., and Gordon, C. H., 1910, The ore deposits of New Mexico: U.S.G.S. Prof. Paper 68.

Lovering, T. S., 1935, Theory of heat conduction applied to geological problems: GSA Bull., v. 46, p. 69–94.

Northrop, S. A., 1959, Minerals of New Mexico: Albuquerque, Univ. of N. Mex. Press, revised edition.

Reiter, M., Edwards, C. L., Hartman, H., and Weidman, C., 1975, Terrestrial heat flow along the Rio Grande rift, New Mexico and southern Colorado: GSA Bull., v. 86, p. 811–818.

Shearer, C., and Reiter, M., 1981, Terrestrial heat flow in Arizona: J. Geophys. Res., v. 86, p. 6249–6260.

Steinhart, J. S., and Hart, S. R., 1968, Calibration curves for thermistors: Deep-Sea Res., v. 15, p. 497–503.

Talmage, S. B., and Wooton, T. P., 1937, The non-metallic mineral resources of New Mexico and their economic features; N. Mex. School of Mines, State Bur. Mines and Mineral Res. Bull. 12.